European Journal of Applied Sciences – Vol. 13, No. 03
Publication Date: June 23, 2025
DOI:10.14738/aivp.1303.18982.
Dakhakhni, T. H., Ahmad, G., & Albaroudi, D. A. (2025). Spectroscopic Investigation of the Neuroprotective Effect of *Lepidium sativum* Water Extract against 2, 4-Dichlorophenoxyacetic Acid Toxicity on Rat Brain Cerebellum Tissue. *European Journal of Applied Sciences*, Vol - 13(03). 406-420.

Spectroscopic Investigation of the Neuroprotective Effect of *Lepidium sativum* Water Extract against 2, 4-Dichlorophenoxyacetic Acid Toxicity on Rat Brain Cerebellum Tissue

Tahani H. Dakhakhni*
Medical Biophysics Lab., King Fahd Medical Research Centre;
King Abdulaziz University

Gehan Ahmed
National Research Centre, Department of Spectroscopy, Egypt

Dalal A. Albaroudi
Medical Lab Department, University Medical Services Centre;
King Abdulaziz University, Saudi Arabia

ABSTRACT

FT-IR spectroscopy is a crucial analytical technique used to study complex structures of biological samples. In the present study, FTIR spectroscopy was applied to verify the neuroprotective effect of Lepidium sativum (LS) water extract against the toxicity of 2, 4-Dichlorophenoxyaceticacid in the cerebellar tissue of rat brains. Treated rats were split into four groups; water control group (water with oral gavage), protective group (LS for 4 weeks then a single dose of 2, 4-D LD_{50}), curative group (a single dose of 2, 4-D LD_{50} then LS for 4 weeks) and LS only group (LS for 4 weeks), a minimum of 5 rats in each group. The group treated with LS alone exhibited a clear recovery from the significant decrease in the protein content after 2, 4-D intoxication, expressed at the amide I band centered at ~1645cm^{-1}. Additionally, significant improvements were observed in the alterations of the secondary protein structure in 2, 4-D intoxicated groups treated with LS extract. Furthermore, notable changes were detected in the looseness of membrane lipid chain packing, lipid polarity and/or a significant rise in the formation of lipids hydroperoxyl groups and carbonyl compounds. However, this effect in the protective group was not as significant as the curative and LS only groups. To conclude, this study demonstrates that LS water extract has a significant potency as an antitoxic/antioxidant effect against neurotoxicity induced by 2, 4-D. Moreover, FT-IR spectroscopy has proven to be rapid and sensitive in toxicity monitoring as well as treatment in biological membranes.

Keywords: Fourier transform infrared spectroscopy (FTIR), Antioxidants, Neurotoxicity, Membrane, Protein, herbicide, FT-IR: Fourier Transform Infrared, LS: Lepidium sativum, 2, 4-D: 2, 4-Dichlorophenoxyacetic acid, LD_{50}: Half lethal dose, LDS: Least square difference, HBW: Half band width, ν: vibrational mode, ν_{as}: Asymmetric vibrational mode

INTRODUCTION

For thousands of years, Plants have been utilized as traditional medicine systems and have continued to offer new remedies to humanity up to this day. Nowadays, plants are known to be the main source of natural antioxidants which may serve as leads for the development of novel drugs (Asraoui et al., 2021). One of the famous medicinal plants is Lepidium sativum (LS), known as garden cress pepperweed, that belongs to the Cruciferae (Brassica) family. The seeds contain protein, fat, carbohydrates, crude fiber (Chatoui et al., 2020), volatile essential aromatic oils, vitamins (β-carotene, riboflavin, niacin, and ascorbic acid), flavonoids and glycosides (Nadkarni 1995). Traditional uses of LS include an analgesic, anti- spasmodic, anti-diarrheal, antimicrobial, antioxidant, anti- inflammatory, hepatoprotective (El-Gendy et al 2023), rapid bone fracture healing, diuretic, galactagogue, hypertension, and renal disease (singh et al., 2022). Previous studies have demonstrated the anticancer action of LS (Suchita Gupta and Reena Gupta 2024). It is believed that this protective effect is thought to result from the presence of polyphenols, that are linked to antioxidant activity and play an important role in stabilizing lipid peroxidation (Yen, Chang, and Duh 2005).

2, 4-Dichlorophenoxyacetic acid (2, 4-D) is a selective, systemic herbicide of the auxin-type (Dakhakhni et al., 2020a). It is commonly used in agricultural to control broad-leaf weeds in cereal crops and is also applied in pastures, lawns, golf courses, and parks (Kaioumova, Süsal, and Opelz 2001). 2, 4-D has been proven to be associated with hepatotoxicity (Dakhakhni et al., 2020b), immunotoxicity (Parizi et al., 2020), teratogenesis (Viriato et al., 2021), neurotoxicity (Ueda et al., 2021) renal toxicity (Shafeeq and Mahboob 2021) and endocrine disruption (Pinto et al., 2024). Several in vitro and in vivo studies on pesticides exposure suggest that high-levels of 2, 4-D have harmful effects on cells, including cell membrane damage (Dakhakhni et al., 2020b) and chromosomal aberrations (Zafra-Lemos et al., 2021).

FT-IR spectroscopy is a powerful physical and chemical technique of great importance used to analyze complex structures of various biological samples. It is an excellent approach that has been demonstrated to be effective in identifying abnormal changes in cells and tissues. Also, it is considered to be a high-throughput, rapid, very sensitive and non-invasive technology capable of precisely detecting even the smallest alterations in bond angels and lengths within molecules functional groups (Dakhakhni et al., 2020a). These alterations can be distinctly represented as a vibrational spectrum from which not only details about the samples' chemical composition can be obtained, but also it provides a comprehensive description of the exact position, area, half band width and height of the IR absorption bands often referred to as a molecular fingerprint. Besides, FTIR spectroscopy has gained exceptional importance due to its low cost, small size, compactness, robustness, lightweight, ease of mass production as well as its ability to analyze a wide range of sample types including liquids, solutions, pastes, powders, films, fibers, gases and surfaces (Dakhakhni et al., 2020a).

MATERIALS AND METHODS

Chemicals and Preparation of *Lepidium sativum* Aqueous Extract

The herbicide 2, 4-D and *Lepedium sativum* seeds were purchased from the local market, Jeddah, KSA. The LD50 dose of 2, 4-D (639mg/kg body weight) was administrated according to (U.S. EPA 2005), while the LS aqueous extract was prepared using the traditional Moroccan

phytotherapy method (decoction). The extract was given orally to different groups of rats at a dose of 20mg/kg body weight (Eddouks et al., 2005).

Experimental Animals

The experimental work of the current study was carried out in the Medical Biophysics Laboratory at the King Fahd Medical Research Center, King Abdul-Aziz University, Jeddah, Kingdom of Saudi Arabia. This study was conducted on twenty male albino Wister rats, provided by the King Fahd Medical Research Center, with a mean initial body weight of 250-350 g. The animals were randomly assigned to groups and housed in plastic cages in a room with a relative humidity of 70%, temperature of 24±1°C, and they were exposed to a 12h light - dark cycle. The treated rats were divided into four groups; the water control group (receiving water via oral gavage), the protective group (receiving LS for 4 weeks followed by a single dose of 2, 4-D LD50), the curative group (receiving a single dose of 2, 4-D LD50 followed by LS for 4 weeks) and the LS only group (receiving LS for 4 weeks). Each group consisted of a minimum of 5 rats.

Infrared Measurement

KBr peletes obtained from the lyophilized samples were measured IR spectrophotometrically according to (Dakhakhni et al., 2020a). Infrared spectra of rats within each group were recorded using a Shimadzu FTIR-8400s spectrophotometer with continuous nitrogen purge. The cerebellum tissue for each single rat was measured triplicate and the IR spectra obtained from different KBr disks were then coadded to represent only one spectrum for each experimental group (Figure 1). Typically, 20 scans were signal-averaged for a single spectrum at a spectral resolution of 4 cm^{-1} in the 3600–445 cm^{-1} spectral range at room temperature. To avoid unavoidable shifts that may arise in the measured spectra, each spectrum was baseline corrected, normalized as normalization produces a spectrum in which maximum value of absorbance becomes 2 and minimum value 0. Furthermore, Normalization to amide I band has also been tested and gave negligible changes in the results. Background spectra were collected under identical conditions and automatically subtracted from the sample spectra. Gaussian components were used to apply the Deconvolution and the best fits for decomposing the bands in the spectral region of interest that were obtained by using Omnic software in order to increase the resolution of the overlapping bands. Proteins and lipids were the parameters of this study.

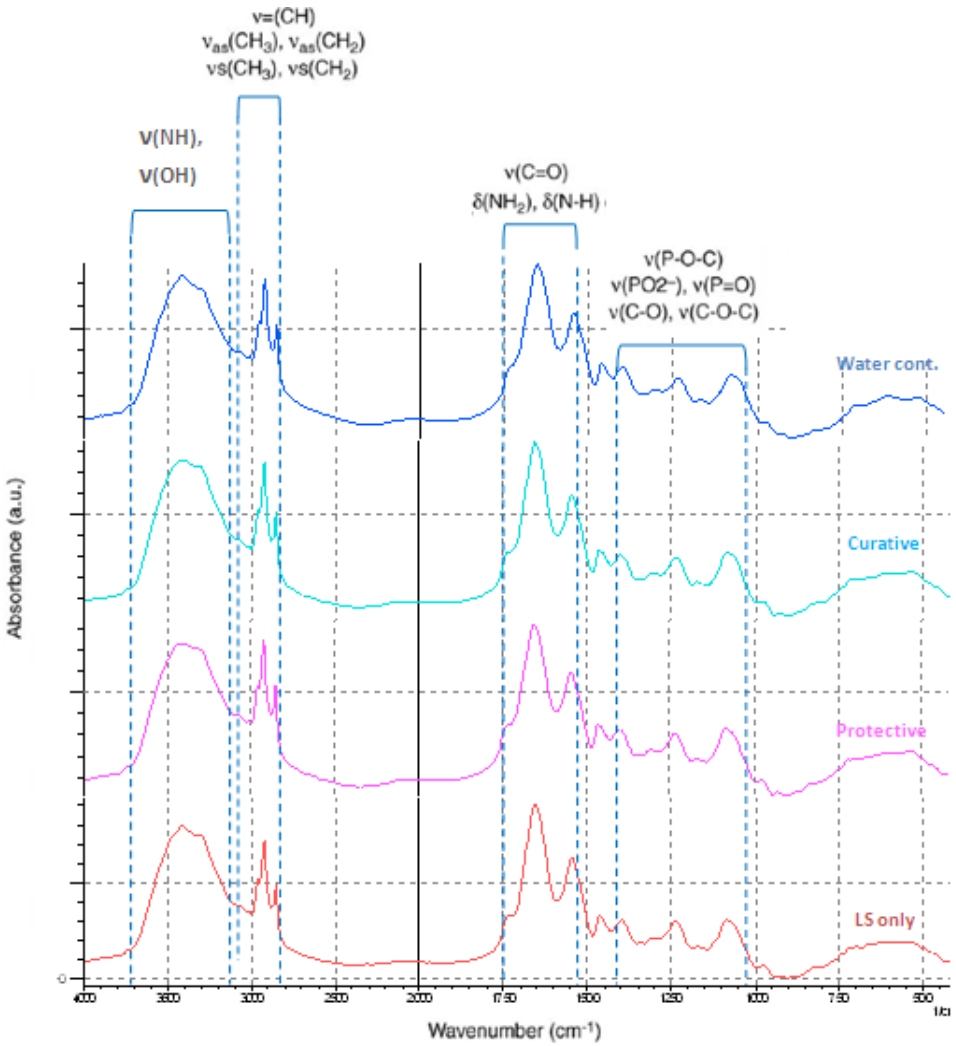

Figure 1: Comparison of the coadded FTIR spectra of water cont. and LS treated groups in the mid infrared region (4000-400 cm^{-1}). Characteristic functional groups contributing to the formation of absorption bands at specific wave numbers are indicated in the Figure.

Statistical Analysis

Some absorbance ratios for bands under investigation, taken from the raw spectra, were calculated and plotted for each different sample. An analysis of variance (ANOVA) test was performed to validate the results obtained from IR measurements. The LSD (Least square difference) test was applied to investigate the significance of the difference between each two groups. Multivariate molecular analysis, namely cluster analysis (with Wards's algorithm method) was conducted using (OMNIC) to interpret similarities or differences between experimental groups under study (Dakhakhni et al., 2020a).

RESULTS

The current study explores the protective and therapeutic effects of LS seeds water extract against neurotoxicity induced by the 2, 4-D herbicide, using FTIR spectroscopy. Particularly, the use of the spectroscopic technique here focuses on the biomolecular changes in protein content, secondary structure, changes in lipid profile and the measurement of lipid

peroxidation or/and the antioxidative effect generated by the 2, 4-D herbicide and the herb LS on rat brain cerebellum.

Infrared Spectral Signature

Infrared spectra were obtained in triplicate from three different rat brain cerebella for each group, then baseline corrected, normalized and overlaid. The main absorption bands in (Figure 1) belonging to lipids, proteins, carbohydrates and nucleic acids were defined in detail together with their assignments according to Corradi et al., (2019) as shown in Table 1.

Three distinct frequency ranges, namely 3600-3050cm^{-1}, 3050-2800 cm^{-1} and 1800-1500 cm^{-1}, were selected to be analyzed in detail.

The Region 3600-3050 cm^{-1}: Analysis of Hydroxyl and Hydroperoxyl Bands

This region is characterized by O-H and N-H stretching vibrations of lipids and proteins. (Corradi et al., 2019). The intensity of the OH stretching bands (3600 cm^{-1} - 3100 cm^{-1}) reflects the degree of lipid oxidation and the amount of hydroxyl-containing lipids such as cholesterol (Corradi et al., 2019), which reflects the levels of the oxidative stress.

Table 1: Proposed assignments of the FTIR spectra of rat brain tissue in the 3600-445cm^{-1} spectral range, according to (Akkas *et al*. 2007; Palaniappan and Vijayasundaram 2009)

Wave number (cm^{-1})	Band assignments
3301	Amide A: mainly **ν**(N–H) of proteins
3072	Amide B: **ν**(N–H) of proteins
3014	Olefinic **ν**(HC=CH): lipids
2956	**νas**(CH_3): mainly lipids
2921	**νas**(CH_2): mainly lipids
2873	**νs**(CH_3): mainly protein
2852	**νs**(CH_2): mainly lipids
1735	Carbonyl **ν**(C=O): lipids
1654	Amide I: **ν**(C=O) of proteins
1544	Amide II: **δ**(N–H) and **ν**(C–N) of proteins
1462	**δ**(CH_2) stretch: mainly lipids
1396	**νs**(COO^-): fatty acids and amino acids
1236	**νas** (PO^{-2}): mainly phospholipids
1082	**νs**(PO^{-2}): mainly nucleic acids; **ν**(HO–C–H): carbohydrates
1000-455	Fingerprinting region: mainly nucleic acids

ν: stretching vibrations, **δ**: bending vibrations, **s**: symmetric, **as**: asymmetric.

Figure 2 presents the curve-fitting analysis for the groups under investigations. The absorption band areas, frequencies and half band widths (HBW) determined through this analysis are summarized in Table 2. It is well known that the band intensity around 3467 cm^{-1} is sensitive to changes in the number of lipids hydroperoxyl groups formed by oxidation (Van de Voort et al. 1994). The other band intensities are sensitive to lipid hydroxyl groups induced by oxidation

while the amide B band centered around 3066cm^{-1} is an indicator for the protein content in the brain tissue (Corradi et al., 2019).

The water control group showed the lowest 3484 cm^{-1}, 3280 cm^{-1}, 3160 cm^{-1} band areas while the LS only treated group had the highest values of these band areas. The area of amide B was elevated in all LS treated groups compared to the water control group with the protective group being the highest among them. The amide B band centered at 3068.84cm^{-1} position tended to be in a higher frequency in all LS treated groups relative to the water control group.

The ratios Amide A/Amide B, Amide I /$\nu_{as}(CH_2)$, corresponding to the protein content within the tissue, were calculated to confirm these spectral signatures (Table 3). For all LS treated groups, there were marked increases in these protein ratios. The lowest values were observed for the water control group (1.727± 0.07, 1.113± 0.07cm^{-1}) for Amide A/Amide B and Amide I /$\nu_{as}(CH_2)$ ratios, respectively, whereas the LS only treated group exhibited the largest value (1.9549, 1.2642cm^{-1}). It is worth noting here that for the curative group (1.8888, 1.1944cm^{-1}), these ratios were higher than for the protective group (1.7875, 1.1877 cm^{-1}) for Amide A/Amide B and Amide I /$\nu_{as}(CH_2)$ ratios, respectively.

The Region 3050-2800 cm^{-1}: Symmetric and Asymmetric Stretching of Methyl (CH_3) and Methylene (CH_2) Functional Groups

The spectral behavior of the bands centered in this region, which comprise mainly the CH stretching vibrations of hydrocarbon chains in lipids (Corradi et al., 2019), can also be considered as an alternative method to determine peroxide as well as measure the CH stretching bands, because oxidation can result in hydrocarbon lipid chains disordering and subsequently increase the corresponding half-band widths (Rodriguez-Casado et al., 2007).

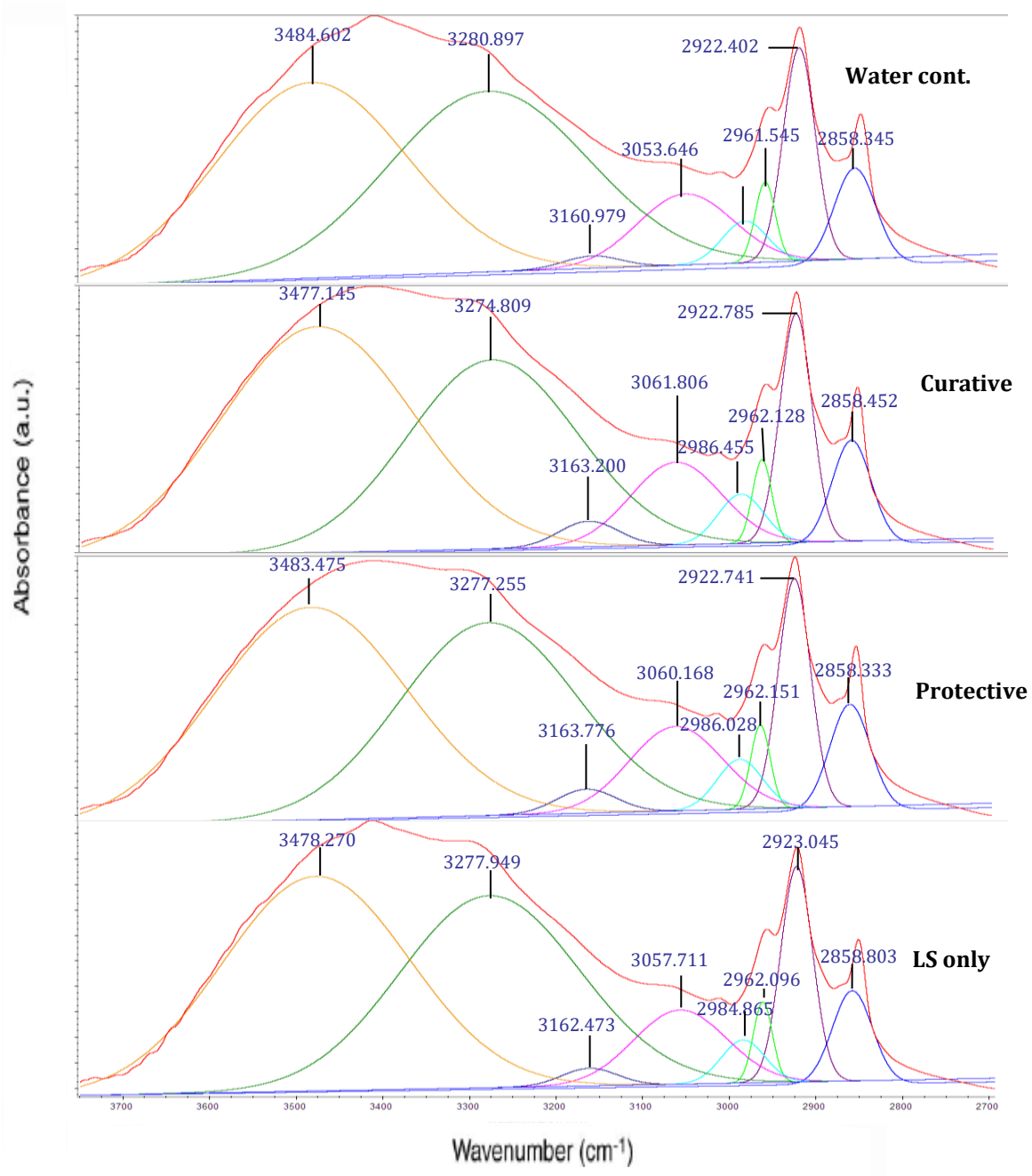

Figure 2: Curve fitting obtained from brain tissues of treated and water control groups in the IR spectral range 3700-2700cm^{-1}

Table 2: Wave numbers, intensities, HBWs and areas of the symmetric and asymmetric stretching of methyl (CH_3) and methylene (CH_2) functional groups associated with lipids in brain tissue.

Groups	Wavenumber (cm^{-1})	Intensity	HBW	Area
Water cont.	2961.545	1.479	27.295	42.973

	2922.402	3.937	43.28	181.398
	2858.345	2.264	56.319	135.73
Curative	2962.128	1.593	26.183	44.389
	2922.785	4.364	43.464	201.885
	2858.452	2.412	53.317	136.884
Protective	2962.151	1.548	26.563	43.762
	2922.741	4.232	44.042	198.402
	2858.333	2.429	55.043	142.327
LS only	2962.096	1.589	25.915	43.836
	2923.045	4.245	43.52	196.653
	2858.803	2.331	54.07	134.144

Primary oxidation products in the treated cerebellum brain sample induce significant changes in the physical state of the lipid acyl chains. These changes are manifested in band shapes, peak heights, half widths, frequency shifts, and integrated intensity of the vibrational bands (Corradi et al., 2019) (Table 2).

The CH_2 band at 2921 showed a marked increase in band area, HBW and intensity for all LS treated groups compared with the water control group. Also, there was a noticeable decrease in the intensity as well as the HBW of the 2858cm^{-1} band for brain tissue of the LS treated groups compared to the water control group.

Table 3: IR intensity absorbance ratios with standard deviation as spectroscopic quantitative measurements of protein content, lipid chain packing, lipid polarity and carbonyl ester formation in rat brain tissue.

Ratios / Groups	Water cont. (a)	Curative (b)	Protective (c)	LS only (d)
Amide A/Amide B I(3303cm^{-1})/I(3072 cm^{-1}) (protein content)	1.7273 ± 0.07^{b,c,d}	1.8888 ± 0.03^{a}	1.7875 ± 0.06^{a}	1.9549 ± 0.08^{a}
Amide I /νas(CH_2) I(1652cm^{-1})/I(2921 cm^{-1}) (protein content)	1.1133 ± 0.07^{d}	1.1944 ± 0.06	1.1877 ± 0.09	1.2642 ± 0.06^{a}
νs(CH_2)/ νs(CH_3) I(2852cm^{-1})/I(2866 cm^{-1}) (lipid chains packing)	1.2237 ± 0.03^{b}	1.2758 ± 0.03^{a}	1.2592 ± 0.04	1.2517 ± 0.03
νas(CH_2) / νs(CH_3) I(2921 cm^{-1}/I(2866 cm^{-1}) (environmental polarity)	1.7563 ± 0.08^{b,c,d}	1.9178 ± 0.05^{a}	1.8378± 0.05^{a}	1.8853 ± 0.06^{a}
ν(C=O) lipids/Amide II I(1735cm^{-1})/I(1547cm^{-1}) (carbonyl formation)	0.5655±0.03^{d}	0.5358 ± 0.01^{c}	0.5626±0.01^{d}	0.523 ± 0.02^{a,c}

Values are means± the standerd diviation (S.D.), for three rats for each group. Significance is at **$p < 0.05$**. Letters are indicative of significance; a= significant against water control group, b=

significant against curative group, c= significant against protective group, d=significant against LS only group.

THE REGION 1800-1500 CM^{-1}: AMIDE I AND CARBONYL BANDS

The data in Table 4 summarizes the positions and fractional percentage areas of the amide I component bands calculated after the best curve-fit for amide I and amide II bands contour of all the tested groups (Figure 3). The positions of these absorptions are influenced by protein conformation. As seen in Table 3, the LS only treated group indicated a higher α-helix area percentage compared to the curative and protective groups. This value (13.97%) is close to the value obtained for the water control group (13.91%). Meanwhile, the curative group (10.35%) had a larger area percentage of α-helix secondary structure than the protective group (7.36%). The total area percentage of both β-sheets and β-turns for all the tested groups are listed in Table 4. It is evident from the Table that the only reduced value of this structure, compared to the water control (64.26%), was detected in the curative group (61.23%).

Table 4: Area percentages of amide I band to determine the changes in the secondary structure of protein in brain tissue. (Heimburg, Esmann and Marsh 1997; Palaniappan and Vijayasundaram 2009)

Wave number(cm^{-1})	Band assignment	Water cont.	Curative	Protective	LS only
1612-1621	β-turns	18.92	20.29	21.11	20.3
1634-1639 / 1641	parallel / unordered structure	21.83	28.41	25.77	19.61
1650-1657	α-helix	13.91	10.35	7.36	13.97
1666-1669	β-turns	31.05	0	34.51	34.37
1672-1677	Parallel β-sheets	1.37	35	0	0
1681-1687	β-sheets	5.45	0.7(1681)-0.28(1685)	0.9(1681)-3.16(1687)	1(1681)-4.41(1687)
1694-1698	Anti-parallel β-sheets	7.47	4.96	7.18	6.33
	Total area β - structure	64.26	61.23	66.86	66.41

The esterified band C=O around 1735 cm^{-1} strongly indicates alteration in the state of intramolecular hydrogen bonding of the interfacial region of the phospholipids structure with water and/or some functional groups of other molecules (Corradi et al., 2019). In the raw FTIR normalized and deconvoluted spectra (Table 5), the carbonyl band splits into three distinct peaks at ~ 1743 cm-1, ~1732 cm-1 and ~1714 cm^{-1}. The total area of these band revealed that the LS only treated group had the minimum area (74.11) while the maximum area (80.551) was determined for the curative group. The area changes followed a decreasing trend in the order: curative > protective > water control > LS only.

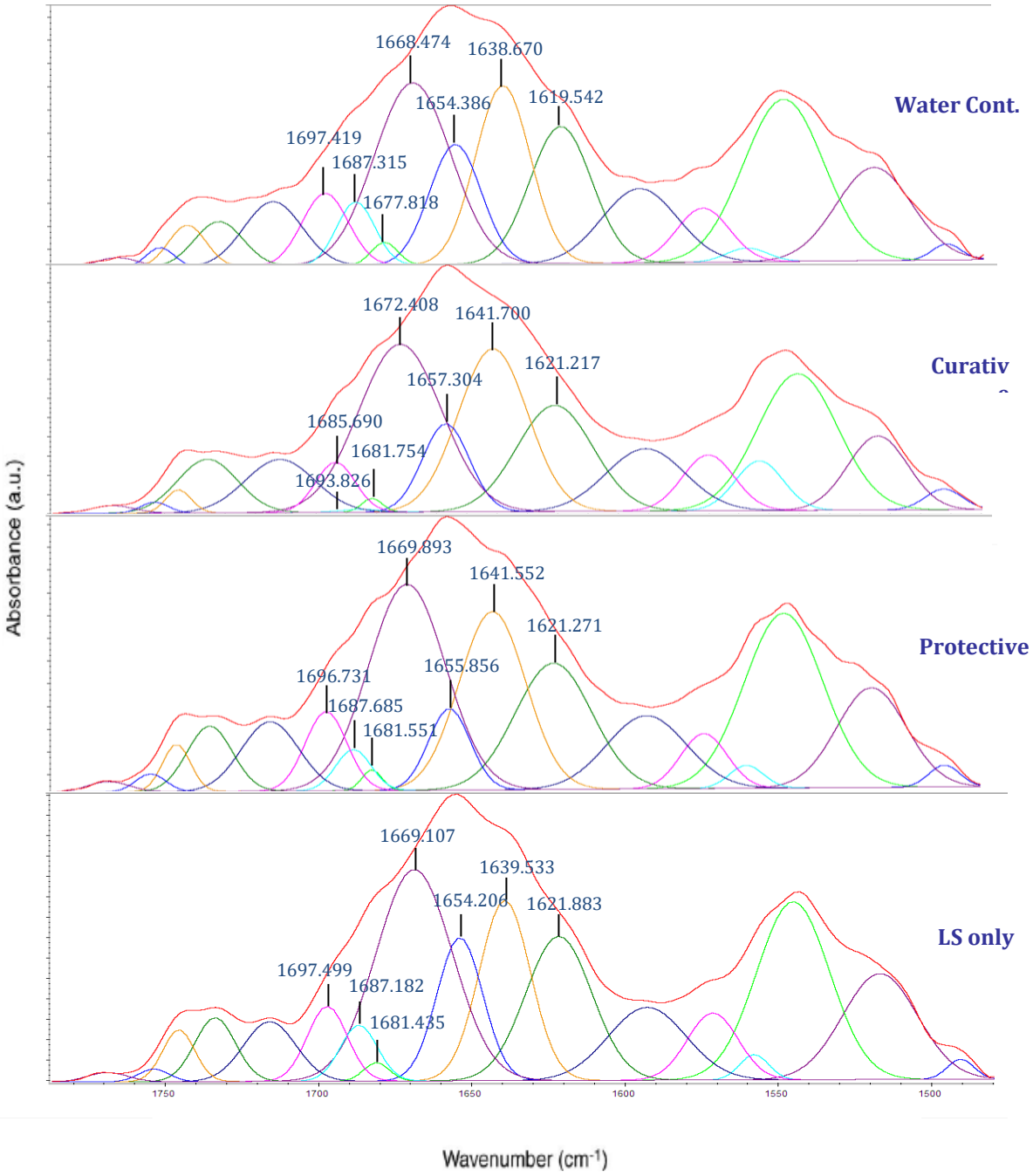

Figure 3: Deconvoluted and peak resolved IR spectra of the brain tissue over the range 1800-1500cm^{-1} for the water control and all LS treated groups.

Moreover, the ratio ν(C=O) lipids/Amide II (1735cm^{-1})/I(1547cm^{-1}) was calculated for all experimental groups (Table 3) as it is an indicative of the weight of formation of carbonyl compounds against lipase action or lipid degradation during lipid oxidation (Shinall et al. 2005). This ratio decreases dramatically in all LS treated groups; the protective group shows a slight decrease in the value of this ratio (0.5626 cm^{-1}), compared to the water control group (0.5655 cm^{-1}). Among the LS treated groups, the lowest value was observed in the LS only treated group (0.523 cm^{-1}).

Table 5: The decomposing of the esterified band C=O around ~1735 cm^{-1}, associated with phospholipids in brain tissue. The table gives the wave numbers, intensities, HBWs and areas corresponding to the resultant curve fitted peaks.

Groups	Wavenumber (cm-1)	Intensity	HBW	Area
Water cont.	1714.684	1.4044	22.6444	33.8513
	1732.613	0.9863	18.9095	19.8522
	1743.047	0.9158	14.5849	14.2184
Curative	1712.227	1.3839	26.9938	39.7657
	1736.213	1.3967	23.1953	34.4865
	1745.83	0.6056	9.7691	6.2975
Protective	1715.306	1.5331	22.4733	36.6749
	1735.349	1.4487	17.6693	27.247
	1746.361	1.0528	10.8922	12.2062
LS only	1716.295	1.4727	19.9982	31.3499
	1734.137	1.5742	15.5085	25.9867
	1746.004	1.2794	12.1836	16.5929

DISCUSSION

Most cells have defense mechanisms against oxidative stress caused by reactive oxygen species (ROS), including superoxide anion, hydrogen peroxide, superoxide radical and hydroxyl radical. These are capable of interacting with proteins, nucleic acids, lipids and/or molecules, altering their structure and ultimately leading to cell damage. This defense includes antioxidants like superoxide dismutase, which converts superoxide anion into hydrogen peroxide and catalase, which converts hydrogen peroxide into water and oxygen. These antioxidants rely on the tendency to donate hydrogen atoms, thus eliminating free radicals. Both Extra- and intracellular antioxidants in nature help maintain balance by controlling excessive radical production and interrupting peroxidative chain reactions (Singh 2019). Unfortunately, we are currently experiencing increased exposure to free radicals due to a number of environmental and pathological conditions. For example, herbicide 2, 4-D has been demonstrated to produce oxidative stress in different doses (Tayeb et al., 2010; Bukowska et al. 2008), leading to neurochemical changes (Rodriguez-Casado et al., 2007). Consequently, endogenous antioxidants may not always be sufficient to counteract excessive exposure to free radicals (Akkas et al., 2007). As a result, numerous studies have focused on the benefits of rich antioxidant nutrition and antioxidant supplements (Singh 2019). With a total phenolic content of approximately 56.3 mg/100 g, LS seeds serve as a valuable source of antioxidants, helping to balance the over production of free radicals (Dakhakhni et al., 2020a). Therefore, the spectroscopic measurement of peroxides in brain tissue samples is of interest to determine levels of oxidative stress and to monitor the protective antioxidant effect.

Peroxide determinations can also be carried out using the 3000-2800 cm^{-1} region, which comprise mainly the CH stretching vibrations of hydrocarbon chains in lipids (Corradi et al., 2019). This is because oxidation may lead to disruption of hydrocarbon lipid chains and subsequent increase of the corresponding half-band widths (Rodriguez-Casado et al., 2007). In this study, the significant broadening (HBW) of the stretching bands of the CH2 groups at 2921 cm^{-1} and 2866 cm^{-1} towards higher frequency in the LS treated groups (Figure 2 and Table 2) over the water control group, means that oxidation increases the lipid chains disordering and

leads to a conversion of lipid hydrocarbon chain trans rotamers to more gauche rotamers, which in turn results in the mentioned band broadening and frequency shift (table 2). These findings align with Corradi et al., (2019) who reported that lower frequencies indicated fewer gauche rotamers and higher hydrocarbon chain order. It is possible that the hydrophobic part of LS, which is the aromatic ring in the phenolic compounds, enters the non-polar part of the membrane, weakens the Van der Waals interactions between acyl chains, and consequently leads to a disordering in the system by raising the number of methylene gauche conformers. In other words, the reduction in the Van der Waals interactions may be responsible for the disordering effect of LS observed in the C–H stretching region of lipids.

Moreover, the observed decrease in frequency of the C=O stretching vibration (~1735 cm^{-1}) (Table 4), might indicate that the O–H group in most of the LS antioxidant components interacts with phospholipids via hydrogen bonding with carbonyl groups, and without interacting with phosphate groups. The results of the current study have provided insight on the LS–membrane interaction and suggest that LS induces a disordering effect on the state-of-order of lipids. From a physiological perspective, this LS-induced disorder might be advantageous because the interaction of antioxidants with lipid radicals is more efficient when membrane lipids are more disordered (Corradi et al. 2019). This finding agrees with the observed increase in the membrane fluidity, indicated by the detected shift in the CH2 band centered at 2922.4cm^{-1} in the water control to 2923.04 cm^{-1} in the LS only group cerebellum spectra (Table 2).

Our protein secondary structures determination results revealed that cerebellum tissues treated with LS only showed a significant increase in the total area percentage of α-helix and β-turns secondary structures with a considerable decrease in β-sheet structure compared to the water control group. Thus, LS administration significantly improves the protein secondary structure in the brain tissues when compared to the water control group. This is considered as an improvement because the decrease in α-helix structure in the cerebellum brain tissues may be responsible for the increase in β-sheet structure, which is consistent with the mechanism of β-sheet formation (Palaniappan, and Vijayasundaram 2009). Furthermore, it was found that the β-sheet structure content in proteins is formed by thermal-, salt- or solvent-induced aggregation (Kim et al., 1994) due to denaturation of proteins. As Raouf et al. 2012 showed, the β-sheet structure in 2, 4-D intoxicated brain tissues suggests that an increase in intermolecular hydrogen-bond interactions lead to the formation of higher molecular weight aggregates, and at the same time modifies the secondary structure of proteins in brain tissues. In addition, examination of the amide I profile for LS curative cerebellum tissues suggests that the overall protein secondary structure contains, to some extent, an α-helix percentage, closely resembles that of the water control cerebellum tissues. These results are consistent with those previously reported by Palaniappan and Vijayasundaram (2009) who studied the arsenic intoxication on brain tissue of Labeo rohita fish.

It should be mentioned here that the therapeutic effect of LS was more beneficial than the protective group. Both groups have a lower content of a-helix and protein secondary structure compared to the water control group (Table 4). Such an antioxidative action of LS is further supported by the dramatic increase in the intensity of amide I protein band that was considerably lower in the brain of the water control (aged rats) group. Thus, these results

revealed that the curative and LS only treated cerebellum tissue had overcome toxicity as well as age-related damage compared to the water control group.

Acknowledgements
Our deep thanks go to Dr. Mohammed Refai for facilitating and guiding rats experiment. Dr. Safa Quisti for reviewing and correcting the paper writing.

Declaration of interest: none.

This research work was supported by King Abdulaziz City for Science and Technology; [grant number: AT-125-18].

References

El-Gendy, M., El-Gezawy, E., Saleh, A., Alhotan, R., Al-Badwi, M., Hussein, E., El-Tahan, H., Kim, I., Cho, S., Omar, S., 2023. Investigating the Chemical Composition of Lepidium sativum Seeds and Their Ability to Safeguard against Monosodium Glutamate-Induced Hepatic Dysfunction. Foods. 12, 4129.

Singh, B., Lubhani, Monzur, M., Sri, M., Ashoor, Kaur, J., Singh, J., 2022. Lepidium sativum: Its nutritional composition and therapeutic properties. The Pharma Innovation Journal. 11(7): 15-25

Gupta, S., Gupta, R., 2024. Research Update on the Therapeutic Potential of Garden Cress (Lepidium sativum Linn.) with Threatened Status. Curr Drug Res Rev.16(3) 369 – 380.

Pinto, T., Guitarte, J., Dias, M., Montagner, C., Espindola, E., González, A., 2024. New insights about the toxicity of 2,4-D: Gene expression analysis reveals modulation on several subcellular responses in Chironomus riparius. Pesticide Biochemistry and Physiology, 204 106088.

Asraoui, F., Kounnoun, A., El Cadi, H., Cacciola, F., El Majdoub, Y., Alibrando, F., Mandolfino, F., Dugo, P., Mondello, L., Louajri, A., 2021. Phytochemical Investigation and Antioxidant Activity of Globularia alypum L. Molecules. 26, 759-771.

Chatoui, K., Harhar, H., El Kamli, T., Tabyaoui, M., 2020. Chemical Composition and Antioxidant Capacity of Lepidium sativum Seeds from Four Regions of Morocco. Evidence-Based Complementary and Alternative Medicine. 4, 1-7.

Corradi, V., Besian I. Sejdiu, Haydee Mesa-Galloso, Haleh Abdizadeh, Sergei Yu. Noskov, Siewert J. Marrink, and D. Peter Tieleman, 2019. Emerging Diversity in Lipid−Protein Interactions. Chemical Reviews. 119 (9), 5775-5848

Nadkarni'S, K.M., 1995. A focus of tissue necrosis increases renal. Indian materica medica. 1, 736-744.

Dixit, J., Iii, V., Kumar, I., Palandurkar, K., Giri, R., and Giri, K., 2020. Lepidium sativum: Bone healer in traditional medicine, an experimental validation study in rats. Journal of family medicine and primary care. 9(2), 812–818.

Tahraoui, A., El Hilaly, J., Israili, Z.H., Lyoussi, B., 2007. Ethnopharmacological survey of plants used in the traditional treatment of hypertension and diabetes in south-eastern morocco (errachidia province). Journal of Ethnopharmacology. 110, 105–117.

Mahassni, S.H., Al-Reemi, R.M., 2013. Apoptosis and necrosis of human breast cancer cells by an aqueous extract of garden cress (Lepidium sativum) seeds. Saudi Journal of Biological Sciences. 20(2), 131-9.

Yen, W.J., Chang, L.W., Duh, P.D., 2005. Antioxidant activity of peanut seed testa and its antioxidative component, ethyl protocatechuate, Lebensm. Wiss. Technol. 38, 193–200.

Dakhakhni, T.H., Raouf, G.A., Qusti SY., 2020a. Investigation of 2, 4-D Hepatotoxicity and Lepidium sativum Antitoxicity on Rat Tissue using FT-IR Spectroscopy. International Journal of Animal Biotechnology and Applications. 6(1), 17–29.

Kaioumova, D., Süsal, C., Opelz, G., 2001. Induction of apoptosis in human lymphocytes by the herbicide 2, 4-dichlorophenoxyacetic acid. Human Immunology. 62, 64-74.

Tayeb, W., Nakbi, A., Trabelsi, M., Attia, N., Miled, A., Hammamia, M., 2010. Hepatotoxicity induced by sub-acute exposure of rats to 2, 4-dichlorophenoxyacetic acid-based herbicide "désormone lourd". Journal of Hazardous Materials. 180, 225-33.

Parizi, J.L.S., Tolardo, A.J., Lisboa, A.C.G., 2020. Evaluation of buccal damage associated with acute inhalation exposure to 2, 4-dichlorophenoxyacetic acid (2, 4-D) in mice. BMC Vet Res. 16, 244.

Viriato, C., França, F.M., Santos, D.S., Marcantonio, A.S., Badaró-Pedroso, C., Ferreira, C.M., Evaluation of the potential teratogenic and toxic effect of the herbicide 2, 4-D (DMA® 806) in bullfrog embryos and tadpoles (Lithobates catesbeianus). Chemosphere. 266, 129-135.

Ueda, R.M.R., de Souza, V.M., Magalhães, L.R., Chagas, P.H.N., Veras, A.S.C., Teixeira, G.R., Nai, G.A., 2021. Neurotoxicity associated with chronic exposure to dichlorophenoxyacetic acid (2, 4-D) - a simulation of environmental exposure in adult rats. J Environ Sci. Health B. 1-11.

DeQuattro, Z.A., Karasov, W.H., 2016. Impacts of 2, 4-dichlorophenoxyacetic acid aquatic herbicide formulations on reproduction and development of the fathead minnow (Pimephales promelas). Environmental Toxicology. 35(6), 1478-1488

Shafeeq, S., Mahboob, T., 2021. 2, 4-Dichlorophenoxyacetic acid induced hepatic and renal toxicological perturbations in rat model: Attenuation by selenium supplementation. Toxicol Ind Health. 37(3), 152-163.

Dakhakhni, T.H., Raouf, G.A., Awatef, A., 2020b. Electron Microscopic Study of Hepatotoxicity Induced by 2, 4-Dichlorophenoxyacetic Acid in Rats. International Journal of Cell Biology and Cellular Processes. 6(2), 18–22.

Zafra-Lemos, L., Cusioli, L.F., Bergamasco, R., Borin-Carvalho, L.A., Portela-Castro, A., 2021. Evaluation of the genotoxic and cytotoxic effects of exposure to the herbicide 2,4-dichlorophenoxyacetic acid in Astyanax lacustris (Pisces, Characidae) and the potential for its removal from contaminated water using a biosorbent. Mutat Res. 865, 503-520.

U.S. EPA, 2005. Reregistration Eligibility Decision for 2, 4-D, NewYork: U.S.

Eddouks, M., Maghrani, M., Zeggwagh, N.A., Michel, J.B., 2005. Study of the hypoglycaemic activity of lepidium sativum l. Aqueous extract in normal and diabetic rats. J. Ethano. Pharmacol. 97, 391–395.

Akkas, S.B., Severcan, M., Yilmaz, O., Severcan, F., 2007a. Effects of lipoic acid supplementation on rat brain tissue: An ftir spectroscopic and neural network stud. Food Chemistry. 105, 1281–1288.

Palaniappan, P., Vijayasundaram, V., 2009. The FTIR study of the brain tissue of labeo rohita due to arsenic intoxication. Microchemical J. 91, 118-124.

Balan, V., Cosmin-Teodor, M., Florina-Daniela, C., Cristina-Mariana, U., Gianina, D., Doru, B., Ioannis, G., 2019. Vibrational Spectroscopy Fingerprinting in Medicine: from Molecular to Clinical Practice. Materials. 12, 2884 – 2825.

Van de Voort, F.R., Ismail, A.A., Sedman, J., Emo, G., 1994. Monitoring the oxidation of edible oils by fourier transform infrared spectroscopy. J Am Oil Chem Soc. 71, 243–253.

Rodriguez-Casado, J., Alvarez, M.I., De Miguel, E., Toledano, A., Carmona, P., 2007. Amphetamine effects on oxidative stress and formation of proteic beta-sheet structures as revealed by ftir microspectroscopy. Biopolymers. 86, 437-446.

Shinall, H., Song, E.S., Hersh, L.B., 2005. Susceptibility of amyloid beta peptide degrading enzymes to oxidative damage: A potential alzheimer's disease spiral. Biochemistry. 44, 15345–15350.

Singh, A, Kukreti, R., Saso, L., Kukreti, S., 2019. Oxidative Stress: A Key Modulator in Neurodegenerative Diseases. Molecules. 24(8), 1583. https://doi.org/10.3390/molecules24081583

Bukowska, B., Rychlik, B., Krokosz, A., Michalowicz, J., 2008. Phenoxyherbicides induce production of free radicals in human erythrocytes: Oxidation of dichlorofluorescine and dihydrorhodamine by 2, 4-d-na and mcpa-na. Food Chem. Toxicol. 46, 359–367.

Kim, Y., Rose, C.A., Liu, Y., Ozaki, Y., Datta, G., Ut, A.T., 1994. FTIR and near-infrared ft-raman studies of the secondary structure of insulinotropin in the solid state: A-helix to β-sheet conversion by phenol and/or high shear force. J. Pharm Sci. 83, 1175–1180.

Raouf, G.A., Qusti, S.Y., Ali, A.M. Dakhakhni, T.H., 2012. The mechanism of 2, 4-dichlorophenoxyacetic acid neurotoxicity on rat brain tissue by using FTIR spectroscopy. *Life Science Journal*, *9*(4), 1686-97.